Effect of age on burst firing characteristics of rat hippocampal pyramidal cells

Anne C. Smith,[1] Jason L. Gerrard, Carol A. Barnes, Bruce L. McNaughton[CA]

Arizona Research Laboratories, Division of Neural Systems, Memory and Aging, Life Sciences North Building, Rm 384, University of Arizona, Tucson, AZ 85724, USA
[1]Present Address: Statistics Research Laboratory, Department of Anesthesia and Critical Care, 55 Fruit St, Clinics 3, Massachusetts General Hospital, Boston, MA 02114, USA

[CA]Corresponding Author

Received 22 August 2000; accepted 28 September 2000

During behavior, hippocampal pyramidal cells emit high frequency bursts, modulated by the animal's location and the 7 Hz theta rhythm. During rest, CA1 EEG exhibits large irregular activity (LIA), containing sharp-wave/ripple complexes, during which pyramidal cells exhibit burst discharge. Aging results in altered intracellular calcium homeostasis, increased electrical coupling and reduced cholinergic modulation within CA1, all of which might affect burst discharge characteristics. During LIA, old rats exhibited more short (3–7 ms) inter-spike intervals, with no change in mean firing rate. During behavior induced theta rhythm, however, interval distributions were not affected by age. Thus, different mechanisms must underlie burst discharge in theta and LIA states. Moreover, age related changes in the cholinergic system appear not to play a major role in shaping the temporal discharge characteristics of CA1 pyramidal cells. The mechanism and significance of the higher frequency bursting in old rats during LIA remains to be determined. *NeuroReport* 11:3865–3871 © 2000 Lippincott Williams & Wilkins.

Key words: CA1; interspike interval; neural ensembles; Sleep; Sharp waves

INTRODUCTION

A variety of neurobiological changes occur during the course of a normal life span. Extensive electrophysiological experiments, however, suggest that the aging process within the hippocampus is not one of general deterioration, but rather exhibits selectivity in terms of process, subregions and cell types [1]. One well characterized change that occurs within CA1 pyramidal cells is an increase in intracellular calcium concentration [2–4]. This increase appears to result from an increase in the number of voltage-gated Ca^{2+} channels (VGCCs) [2,3], although the single L-channel kinetics are not altered. Due to the increased calcium current, old pyramidal cells also show larger afterhyperpolarizing potentials (AHP) [5–7]. Because VGCCs are strongly activated during complex-spike bursting [8] that occurs during quiet waking or slow wave sleep states when the hippocampal EEG exhibits LIA, the firing characteristics of aged pyramidal neurons might be altered under these conditions. In addition, other cellular processes may contribute to cell activity changes during aging, including changes in membrane ion pumps or intracellular buffering [4], increased gap junctional connections [9] and changes in cholinergic modulatory mechanisms [10].

Hippocampal CA1 pyramidal cells, in freely behaving rats, fire selectively in specific regions of environments [11]. Within the place field of a given pyramidal cell, the cell fires in high frequency bursts that are modulated by both location and phase of the local EEG theta rhythm. Interestingly, the ensemble firing patterns of pyramidal cells that occur during awake exploration are reactivated during subsequent rest periods (quiet wakefulness and slow-wave sleep), particularly during the ~50 ms sharp-wave EEG events that occur in these behavioral states [12]. It has been proposed that this reactivation may play a role in the memory consolidation process [12–14].

Sharp-waves are accompanied by high-frequency ripple oscillations near the CA1 pyramidal layer and high-frequency, complex-spike bursts in the pyramidal cells, which are apparently mediated by calcium currents [8]. Burst discharges in both LIA and theta states have similar frequency characteristics, and are accompanied by a progressive failure of dendritic invasion of the sodium spike, which often results in an attenuation of the extracellularly recorded spike [15]. This has led to the suggestion that the bursts in the two states share a common mechanism [16].

Although mean firing rates during behavior do not differ between age groups [17], changes in calcium homeostasis and other cellular parameters that occur in aged animals could affect the frequency characteristics of burst discharge, in the absence of changes in overall mean rate. This study, therefore, addressed the effect of age on the firing characteristics of extracellularly recorded pyramidal neurons and the corresponding EEGs during rest epochs and behavior. Some of these data have been reported previously in abstract form [18].

MATERIALS AND METHODS

Seven aged Fischer F344 male rats (25–31 months) and seven young male rats (11–12 months) were used in this study. The experimental procedures were approved by the University of Arizona Institutional Animal Care and Use Committee and all researchers were certified in the care and use of research animals, in accordance with local and federal guidelines. Each rat was housed individually in a Plexiglas guinea pig tub and maintained on a reversed 12:12 h light:dark cycle. During training and recording, the rats were maintained at 80% *ad lib* body weights, had free access to water, and were handled and weighed daily.

A multielectrode microdrive assembly (hyperdrive) [19] consisting of 14 independently movable probes, was implanted over the right hippocampus in order to acquire extracellular spike signals from multiple single cells in the CA1 layer. All surgical procedures were performed in accordance with NIH guidelines. Twelve of the probes were tetrodes used for single unit recording. One of the two additional electrodes was placed in the corpus callosum and used as a differential reference. The other was placed near the hippocampal fissure, to record theta rhythm in the EEG. NIH guidelines were followed for all surgical procedures. EEG data were recorded from one channel of each of the 12 single-unit tetrodes and sampled at 1 kHz. Light-emitting diodes were attached to the headstage to track the location of the rat via a ceiling mounted camera. The principle of tetrode recording is an extension of the stereotrode recording method and has been described in detail previously [20].

The general experimental design included three phases: (1) a rest session, during which the rat rested quietly and slept in a towel-lined pot for 30–60 min (PRE-Rest), (2) a behavior session, in which the rat traversed a track for 20–30 min for food reward, and (3) a final rest session in which the rats were placed back into the pot and were allowed to rest quietly and sleep for an additional 30–60 min (POST-Rest). Five of the seven old rats and five of the seven young rats ran on a rectangular track (94×43 cm) during the maze running session. The remaining two young and two old animals ran on a T-maze track. The T-maze experience included interspersed forced choice turns and free choice turns with the two ends of the T-maze food rewarded differentially (80% and 20%).

Data were analyzed from 22 recording sessions for young rats, and 17 sessions from old rats, averaging 18 cells per session per animal. Cells were identified using an off-line, manual clustering program (Xclust, M.A. Wilson or Mclust, A.D. Redish) and classified as either pyramidal cells or interneurons depending on their spike duration and firing rate characteristics. A small percentage of all neurons ($< 5\%$), which were not classified as interneurons, but fired at a rate < 0.03 Hz or > 5 Hz during 5 min of behavior were excluded. The final data set consisted of 392 cells from the young rats and 390 cells from the old rats. Rest epoch statistics were based on 15 min time periods immediately before (PRE) or immediately after (POST) behavior on the track, and the interspike intervals from the behavior epochs were generated from five minutes of track running data. Twelve EEG recordings from seven young rats and nine EEG recordings from six old rats were included in the analysis; EEG data from one old rat were discarded due to a computer malfunction during recording. The raw EEGs were compared using their power spectral density (psd) generated using Welch's averaged, modified periodogram method [21]. For the purposes of comparison, the psds were normalized by the total power in the signal between 0 and 500 Hz and then plotted on a log scale.

The global state of the hippocampus is different during locomotion and other attentive behaviors, when the EEG is dominated by the theta rhythm, and during off-line periods such as sleep or quiet wakefulness, when the EEG displays large irregular activity and sharp wave/ripple complexes [15]. Sharp waves are initiated by a population burst in CA3, which projects feedforward excitation onto both pyramidal cells and interneurons in the CA1 layer [15]. The large excitation of both pyramidal cells and interneurons produces a high frequency oscillation ($\sim$200 Hz) called a ripple within the CA1 layer. Rest EEG data were filtered from 6 to 10 Hz to identify theta, and from 100 to 300 Hz to identify high frequency ripples, indicative of sharp-wave activity. These filters were used to classify the EEG data in order to ensure that no data containing theta rhythm were included in the rest sessions. Experimenter notes from the recording sessions were also used to remove time periods from the rest data when the animal was seen to be awake and active. Conversely, the behavior EEG data were filtered from 100 to 300 Hz and classified to ensure that no sharp waves were included in the behavior data. Thus, the LIA (rest) data were not contaminated with theta (awake behavior) states and vice versa. Where data segments were removed by this screening process, the corresponding intervals were omitted.

The ISI distributions for each rat were calculated by averaging the interspike intervals for all pyramidal cells recorded from each rat. Each cell's ISI distribution was normalized by the total number of interspike intervals before averaging across each animal. Specifically, each cell's distribution was generated by summing the number of ISIs in 0.5 ms bins and then dividing by the total number of intervals. Hence, for each cell, the integral under the distribution is unity. The third moments (skewness) were computed for all ISI distributions from each rat, normalizing by the total number of interspike intervals in the range from 0 to 100 ms. The skewness values were used to compare ISI distributions within the 0–30 ms range. Skewness is dimensionless measure of asymmetry within a distribution, and is defined here for a distribution of values $\{x_j\}$ by the expression [22]

$$\frac{1}{N}\sum_{j=1}^{N}\left[\frac{x_j - \bar{x}}{\sigma}\right]^3$$

where $\sigma = \sigma(x_1,...x_N)$ is the standard deviation of the distribution and is the median of the distribution. All of the ISI distributions tended to be positively skewed (long tail on the right), with the larger skewness values corresponding to a long right tail in the distribution and an increased left shift in the values within the distribution, relative to a normal distribution. Increased skewness thus corresponds to an increase in the relative proportions of short ISIs.

RESULTS

Figure 1 shows the mean and s.e. for the interspike interval distribution of all 782 pyramidal cells from both age groups over the interval 0–100 s in the LIA (PRE-Rest, Fig. 1a) and theta (Behavior, Fig. 1c) states. Because most of the distribution lies on a short time scale and we are interested in the brief interspike intervals that tend to occur during bursts, the analysis was limited to the time interval from zero to 30 ms. The ISI distributions from zero to 30 ms includes ~40% of the total number of interspike intervals. Figure 1b shows ISI distributions representative of the mean measured during rest for an individual young and old rat during PRE-Rest. For each animal, the mean (± s.e.m.) ISI over all the cells recorded from that animal is shown. Note that the old rat has a larger percentage of ISIs in the 3–7 ms range than does the young rat, i.e. the distribution displays a higher peak in the short ISIs for the old rat relative to the young rat. Figure 1d shows ISI distributions representative of the mean measured during track running for the same individual young and old rats during Behavior in the 0–30 ms range. Note that the distributions for the two animals are similar in this behavioral state.

Figure 2 shows the mean and SEM of the ISI distribu-

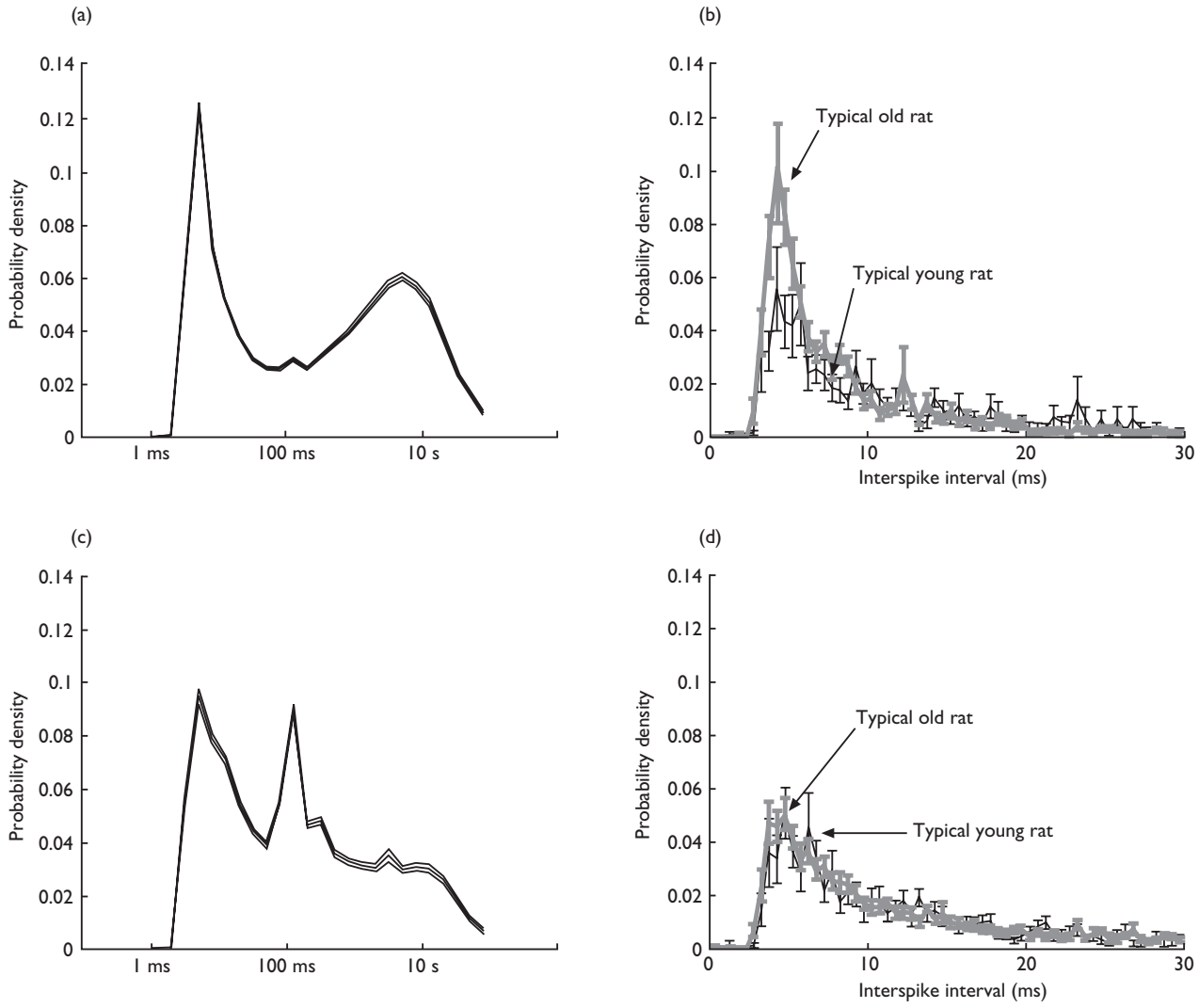

Fig. 1. (**a**) Interspike interval (ISI) distribution averaged over all 782 cells in the time range from 0 to 100 s (the x axis is $\log_{10}$ ISI) for the PRE-rest data. The ISI distribution is plotted as a probability density function; therefore the area under the total curve equals one. Note that the bulk of the distribution is on short time scales with a large peak around 4 ms. (**b**) Probability density function of interspike intervals for a representative young rat and a representative old rat. The interspike intervals are shown on the short time scale ranging from 0 to 30 ms. These plots display the mean ISI distribution and standard error from all cells recorded in one old and one young rat. (**c**) Interspike interval (ISI) distribution averaged over all 782 cells in the time range from 0 to 100 s (the x axis is $\log_{10}$ ISI) for the Behavior data. (**d**) Probability density function of interspike intervals for a representative young rat and a representative old rat during track running Behavior. The interspike intervals are shown on the short time scale ranging from 0 to 30 ms.

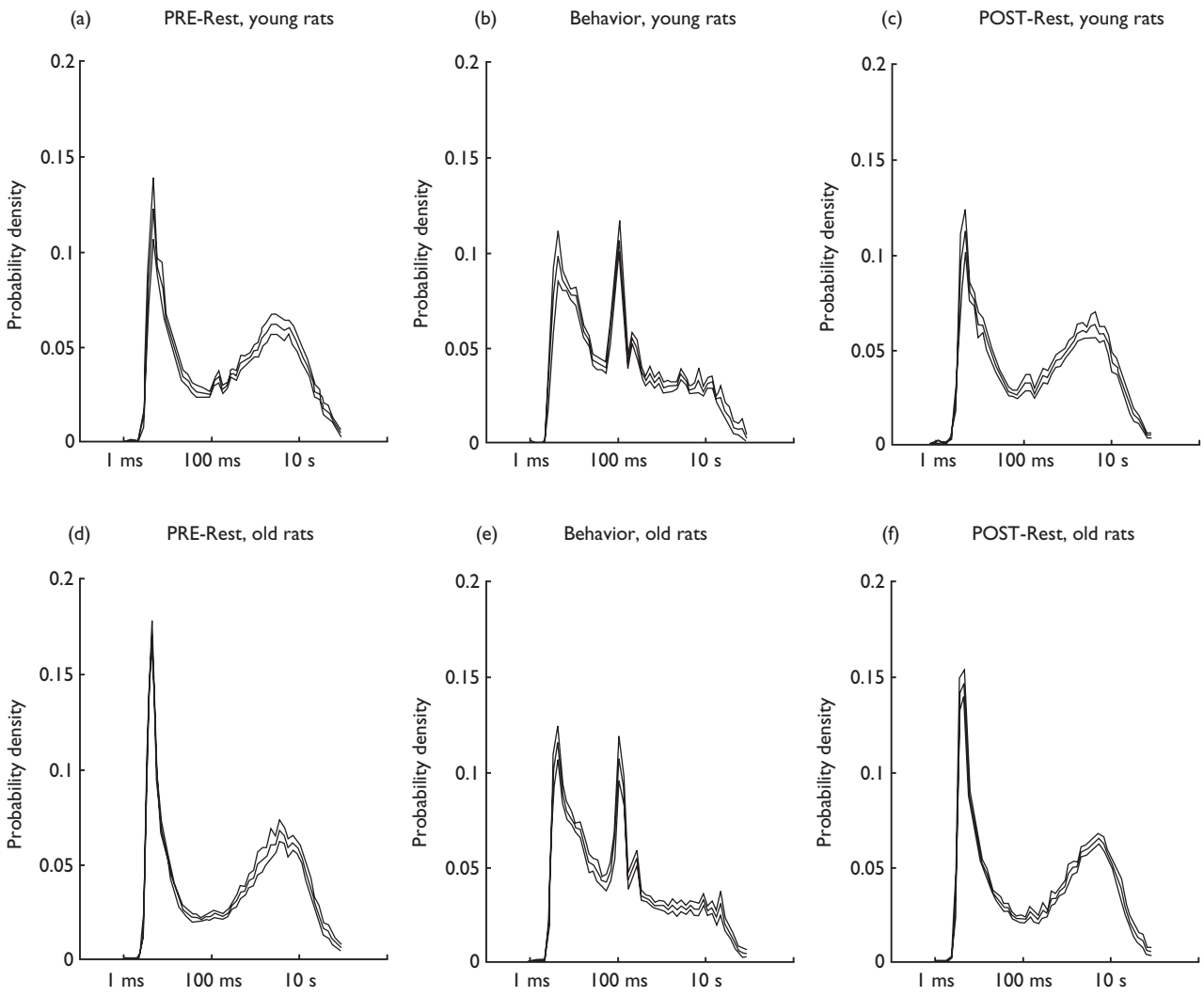

Fig. 2. The mean (and s.e.m.) interspike interval distribution averaged across all days in each animal is shown during rest epochs and track behavior out to 100 s (the x axis is $\log_{10}$ ISI). (**a**) PRE-Rest in young rats. (**b**) Track running (Behavior) in young rats. (**c**) POST-Rest in young rats. (**d**) PRE-Rest in old rats. (**e**) Track running (Behavior) in old rats. (**f**) POST-Rest in old rats.

tions averaged across rats in each age group for intervals out to 100 s. Figure 2a,d, illustrates the differences in interspike interval distributions during the rest period before track running between age groups. Note the ISI distribution for the old rats is narrower and higher in the 3–7 ms range. The mean skewness over the 0–30 ms time interval for young and old rats in PRE-rest is 2.12 ± 0.10 and 2.39 ± 0.05, respectively ($p < 0.05$, Student's t-test). These significant age differences are observed under various conditions, i.e., the age effect persists when the time interval is varied from 0 to 15 ms or 0 to 45 ms and is independent of whether median or mean is employed in the formula for skewness. In contrast, Fig. 2b,e shows that there is no difference between age groups in the interspike interval distributions during theta rhythm, when the rats are locomoting on the tracks ($p > 0.20$). Figure 2c,f shows the mean and s.e.m. of the ISI distributions during the POST-Rest epoch, for young and old rats, respectively. Again, this illustrates the tendency for old rats to show a larger proportion of interspike intervals in the 3–7 ms time range (within the complex spike burst interval times). Figure 3 focuses on the 0–15 ms range during each of these behavioral states, to allow closer inspection of the differences between age groups in the PRE-Rest (a and c for young and old rats, respectively) and POST-Rest (c and e for young and old rats, respectively) epochs, and the lack of difference between age groups during track running behavior (b and d for young and old rats, respectively).

Figure 4 displays the skewness in the ISI distribution averaged across all cells recorded from each animal in both

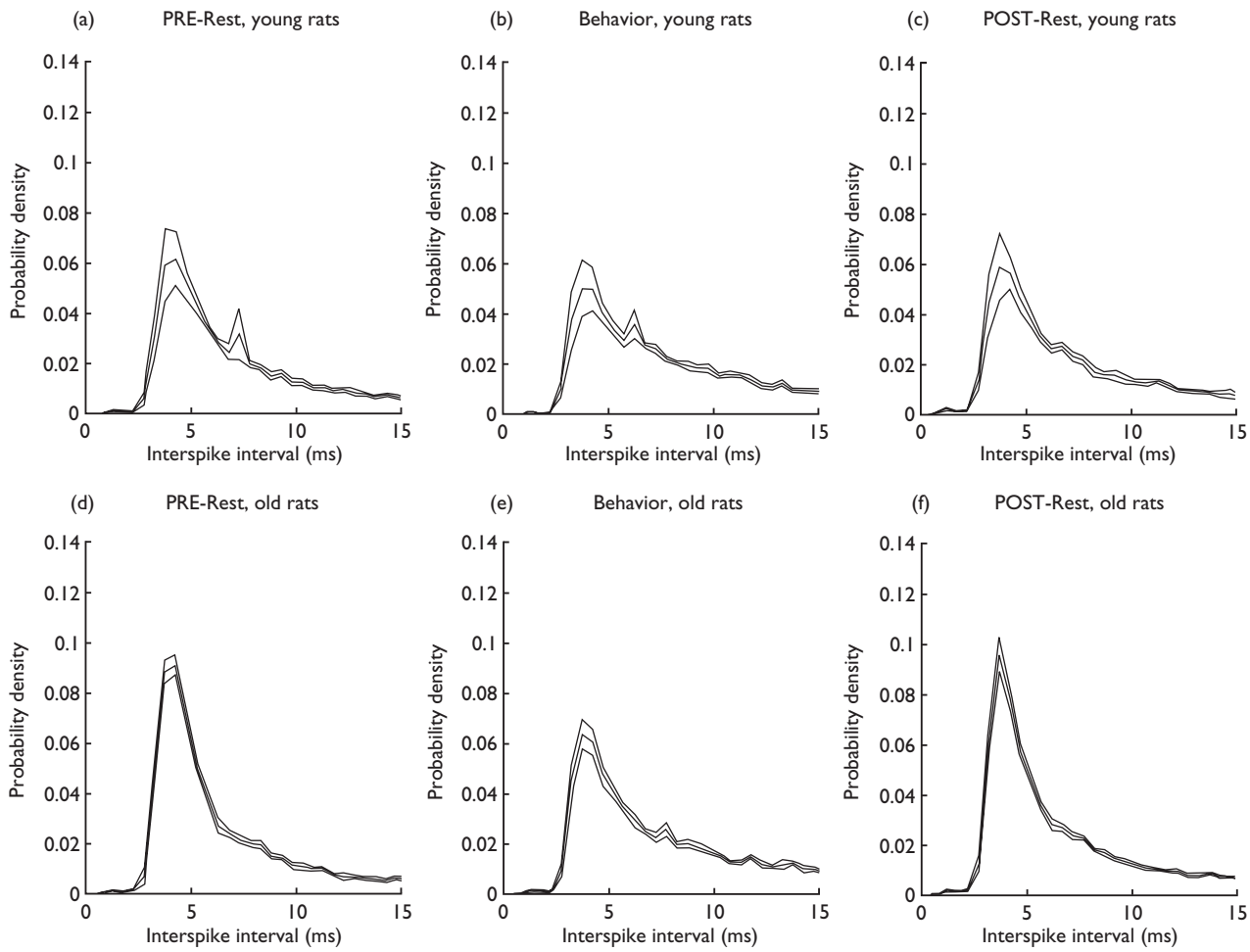

Fig. 3. The mean (and s.e.m.) interspike interval averaged across all days in each animal is shown during rest epochs and track behavior from zero to 15 ms. (**a**) PRE-Rest in young rats. (**b**) Track running (Behavior) in young rats. (**c**) POST-Rest in young rats. (**d**) PRE-Rest in old rats. (**e**) Track running (Behavior) in old rats. (**f**) POST-Rest in old rats.

rest epochs (PRE in Fig. 4a and POST in Fig. 4b) *vs* the corresponding data from Behavior. In both age groups skewness was higher in both rest epochs (PRE and POST), than during track running behavior. The skewness difference between rest and track running, however, was greater in old rats. The aged animals displayed a larger skewness than did the young animals during both rest periods whereas there was no difference between the age groups in the skewness of the ISI distribution during behavior. Interestingly, both young and old rats tended to show slightly greater skewness of the ISI distribution in PRE-Rest than in POST-Rest periods. In 32 of 39 experiments, PRE-Rest skewness was greater than POST-Rest skewness, representing a significant difference between rest epochs for the animals as a whole ($p < 0.05$, two-tailed sign test). Although a number of interpretations are possible, these data suggest that there may have been some effect of the behavioral experience on cell firing characteristics recorded during the rest period after track running.

In addition to the individual cell firing information, EEG data recorded from the same electrodes were also analyzed. Figure 5 shows the averaged power of the EEG at frequencies ranging from zero to 500 Hz for both age groups during PRE-Rest. There was an increase in EEG power at the high end (100–250 Hz) of the frequency spectrum for old rats (the increased high frequency component can easily be observed when viewing the individual EEGs). No significant difference can be observed in the EEG power spectra between the two rest epochs (PRE and POST) for either age group (data not shown).

DISCUSSION

During rest (LIA), aged rats exhibit pyramidal cell spike trains with ISI distributions that are significantly more left-

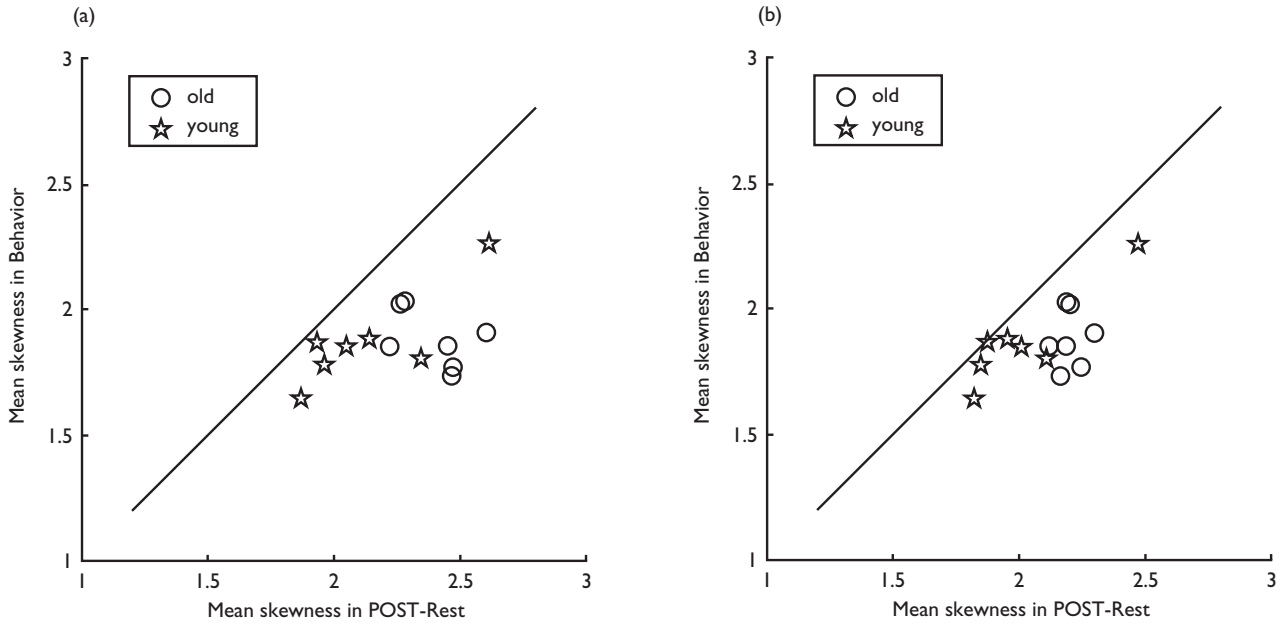

Fig. 4. The mean (and s.e.m.) interspike interval distribution skewness value, averaged across all days in each rat, is shown during track running behavior and during the two rest epochs. The data points shown as open circles represent each aged animal and the stars represent each young animal. (**a**) PRE-Rest *vs* behavior. (**b**) POST-rest *vs* behavior. The skewness is higher for the aged animals in both PRE-Rest (a) and POST-Rest (b), which is indicated by the tendency for the skewness values in young rats to fall closer to the origin in both PRE- and POST-Rest. Also the interspike interval distribution is more skewed in both Rest epochs than during Behavior, shown by all the data points lying to the right of the line.

skewed compared to young rats. This occurs in spite of the fact that there is no age difference in the mean spike rate. Thus, in the LIA state, either the average interspike interval (ISI) during a complex spike burst is shorter or spikes are more concentrated within complex spike bursts in old rats. The altered ISI distribution cannot be explained by changes in the duration of sharp waves or their frequency of occurrence, which did not differ between age groups [23]. There was, however, a significant increase in the power at higher (100–300 Hz) frequencies in EEG of the old animals relative to the young animals. This frequency range corresponds to the so-called ripple oscillation that is observed near the pyramidal cell layer during sharp wave events [15]. Because pyramidal cell firing tends to be phase locked with these oscillations [15], this effect is consistent with the observed decreased interspike intervals during the complex spike burst in old animals, and the two effects likely share a common underlying mechanism.

The alteration in pyramidal cell firing characteristics might be explained by a variety of changes in the function of hippocampal cells that are known to occur with ageing. Although the number of CA1 pyramidal cells is preserved in ageing rats [24], there is evidence that overall calcium homeostasis within these cells is altered. In particular, the density of single L-type calcium channels increases with age [2,3], which results in larger calcium action potentials and increased post-burst afterhyperpolarizing potentials (AHPs) [5–7]. Aged pyramidal cells also exhibit an increased spike frequency accommodation to prolonged depolarizing stimuli *in vitro* [7]. The combination of these changes could alter the excitability characteristics of old pyramidal cells, creating conditions which favor more within burst action potentials during sharp waves and fewer single action potentials between sharp wave-induced bursts. In addition, CA1 pyramidal cells in the aged hippocampus possess a greater number of gap junctional connections with neighboring cells than do young CA1 pyramidal neurons [9]. This increased electrical communication between pyramidal cells may also increase the spread of burst firing within the network. A combination of these age-dependent alterations in cellular biophysical properties, could contribute to the interspike interval changes.

Old rats also show substantial reductions in functional cholinergic transmission in the hippocampus [10]. Thus, an age difference may have been expected during behavioral states in which the cholinergic system is engaged; however, no age difference arose during behavior. These data imply either that the cholinergic system does not play a major role in shaping the temporal discharge characteristics of CA1 pyramidal cells during behavior, or that the cholinergic system effects are saturated at low input values.

A comparison between the ISI distributions recorded during rest epochs and behavior (Fig. 1, Fig. 2 and Fig. 3) show that shorter interspike intervals are more prevalent during rest than during behavior in both age groups.

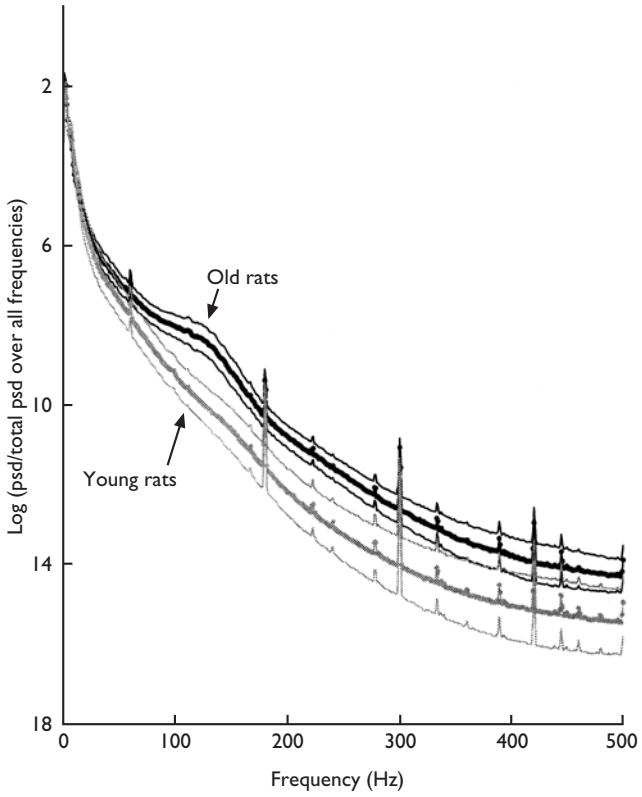

Fig. 5. Comparison of the mean power spectra in EEG taken from 15 min of PRE-Rest for both old (gray) and young (black) rats while the rats were in the LIA state. The normalized power spectral density, on a log scale, is plotted against frequency, showing the mean and standard error of the mean for each age group. Results are taken from the average across nine datasets from six old rats and the average across 12 datasets from 7 young rats. Data were averaged within each rat before the mean was determined within an age group. Note the difference between the age groups in the power spectrum of the EEG in the range of 100–250 Hz.

Although the interspike intervals during LIA are reduced in aged animals, there was no effect of age on interspike interval distributions during behavior when the EEG exhibits theta rhythm. This implies that, contrary to a recent suggestion [16], the burst mechanisms of pyramidal cells are different between rest and active behavioral states.

The fact that the age difference only appears during rest, and not during track running, suggests that old hippocampal pyramidal cells are able to maintain normal firing dynamics while the rat is engaged in active behavior. Whether the altered firing characteristics during LIA are of functional significance with respect to information processing (e.g., memory consolidation) remains to be determined.

REFERENCES

1. Barnes, CA. *Trends Neurosci* **17**, 13–18 (1994).
2. Landfield PW. *Life Sci* **59**, 379–387 (1996).
3. Thibault O and Landfield PW. *Science* **272**, 1017–1020 (1996).
4. Biessels G and Gispen WH. *Life Sci* **59**, 379–387 (1996).
5. Landfield PW and Pitler TA. *Science* **226**, 1089 (1984).
6. Moyer JR, Thompson LT, Black JP and Disterhoft JF. *J Neurophysiol* **68**, 2100 (1992).
7. Disterhoft JF, Thompson LT, Moyer JR and Mogul DJ. *Life Sci* **59**, 413–420 (1996).
8. Wong RKS and Prince DA. *Brain Res* **159**, 385–390 (1978).
9. Barnes CA, Rao G and McNaughton BL. *J Comp Neurol* **259**, 549 (1987).
10. Shen J and Barnes CA. *Neurobiol Aging* **17**, 439–451 (1996).
11. O'Keefe J and Dostrovsky J. *Brain Res* **34**, 171–175 (1971).
12. Kudrimoti HS, Barnes CA and McNaughton BL. *J Neurosci* **19**, 4090–4101 (1999).
13. Marr D. *Philos Trans R Soc Lond (Biol)* **262**, 23–81 (1971).
14. Buzsaki G. *Neuroscience* **31**, 551–570 (1989).
15. Buzsaki G. *Brain Res* **398**, 242–252 (1986).
16. Quirk MC and Wilson MA. *J Neurosci Methods* **94**, 41–52 (1999).
17. Shen J, Barnes CA, McNaughton BL *et al. J Neurosci* **17**, 6769–6782 (1997).
18. Smith A. *Soc Neurosci Abstr* **26**, in press.
19. Gothard KM, Skaggs WE, Moore KM and McNaughton BL. *J Neurosci* **16**, 823–835 (1996).
20. McNaughton BL, O'Keefe J and Barnes CA. *J Neurosci Methods* **8**, 391–397 (1983).
21. Matlab, The MathWorks, Inc. Natick, MA
22. Press WH, Teukolsky SA, Vetterling WT *et al. Numerical Recipes in C.* Cambridge: Cambridge University Press; 1992, p. 612.
23. Gerrard JL, Kudrimoti HS, Barnes CA and McNaughton BL. *Soc Neurosci Abstr* **22**, 932 (1998).
24. Rapp P and Gallagher M. *Proc Natl Acad Sci USA* **93**, 9926–9930 (1996).

Acknowledgements: This work was supported by Flinn/IGERT Biomathematics Fellowship, MH46823, AG12609, MH01565 and Arizona Chapter of ARCS. We thank Stephen Cowen and Hemant Kudrimoti for their participation in data collection, and Emery Brown and Loren Frank for useful comments during preparation of the manuscript.